THE JOURNAL OF BIOLOGICAL CHEMISTRY
Vol. 276, No. 1, Issue of January 5, pp. 529–534, 2001

Printed in U.S.A.

Tau Filament Formation in Transgenic Mice Expressing P301L Tau*

Received for publication, July 21, 2000, and in revised form, September 15, 2000
Published, JBC Papers in Press, September 29, 2000, DOI 10.1074/jbc.M006531200

Jürgen Götz‡, Feng Chen, Robi Barmettler, and Roger M. Nitsch

From the Division of Psychiatry Research, University of Zürich, 8008 Zürich, Switzerland

Mutations in the microtubule-associated protein tau, including P301L, are genetically coupled to hereditary frontotemporal dementia with parkinsonism linked to chromosome 17. To determine whether P301L is associated with fibril formation in mice, we expressed the longest human tau isoform, human tau40, with this mutation in transgenic mice by using the neuron-specific mouse Thy1.2 promoter. We obtained mice with high expression of human P301L tau in cortical and hippocampal neurons. Accumulated tau was hyperphosphorylated and translocated from axonal to somatodendritic compartments and was accompanied by astrocytosis and neuronal apoptosis indicated by terminal deoxynucleotidyl transferase-mediated biotinylated dUTP nick end-labeling staining. Moreover, P301L tau formed abnormal filaments. Electron microscopy of sarcosyl-insoluble protein extracts established that the filaments had a straight or twisted structure of variable length and were ~15 nm wide. Immunoelcecton microscopy showed that the tau filaments were phosphorylated at the TG3, AT100, AT8, and AD199 epitopes *in vivo*. In cortex, brain stem, and spinal cord, neurofibrillary tangles were also identified by thioflavin-S fluorescent microscopy and Gallyas silver stains. Together, our results show that expression of the P301L mutation in mice causes neuronal lesions that are similar to those seen in human tauopathies.

Hereditary frontotemporal dementia with parkinsonism linked to chromosome 17 is a group of neurodegenerative diseases characterized by early behavioral changes accompanied by subsequent cognitive and motor disturbances. More than a dozen families were identified, with diverse but overlapping clinical features. Pathological changes include selective frontotemporal atrophy, neuronal loss, gliosis, and spongiosis in several brain areas in addition to abundant filamentous inclusions composed of hyperphosphorylated tau protein in neurons and, to some extent, in glial cells (1).

Tau is an axonal, microtubule-associated phosphoprotein in normal adult brain (2). Tau has tubulin-polymerizing activities *in vitro* (3); it establishes short cross-bridges between axonal microtubules and thereby supports functions in intracellular trafficking including axonal transport (4). In neurons affected by tauopathy, tau is hyperphosphorylated and is located not only in axons but also in cell bodies and dendrites (5, 6). Results from *in vitro* studies suggest that disease-causing mutations in the tau gene result either in the reduced ability of tau to interact with microtubules or in increased ratios of four-repeat (4R)[1] to three-repeat tau caused by quantitative changes in the splicing in of exon 10. (7, 8).

To demonstrate that human tau can form filaments in mouse brains and to reproduce aspects of the human pathology, including neurofibrillary tangle formation, in transgenic mice, we expressed the longest isoform of human tau with the frontotemporal dementia with parkinsonism linked to chromosome 17 causing mutation P301L in neurons by using a neuron-specific promoter. Tau accumulated mainly in neurons of the neocortex and hippocampus; it was hyperphosphorylated at distinct sites and formed filaments similar to those present in human tauopathies.

EXPERIMENTAL PROCEDURES

Constructs and Transgenic Mice—By a PCR-mediated approach, the human pathogenic mutation P301L was introduced into the cDNA encoding the longest human brain tau isoform. This isoform contains exons 2 and 3 as well as four microtubule-binding repeats (2^+3^+4R, human tau40). To be able to discriminate P301L tau transgenic from wild-type tau transgenic mice, a silent mutation was introduced into the P301L construct that destroys a diagnostic *Sma*I restriction site. The cDNA was conferred with a Kozak consensus sequence and was subcloned into a murine Thy.1.2 genomic expression vector (Dr. Herman van der Putten, Novartis, Basel, Switzerland). Vector sequences of this construct (named pR5) were removed before microinjection. Transgenic mice were produced by pronuclear injection of B6D2F1 × B6D2F1 embryos. Founders were identified by PCR analysis of lysates from tail biopsies using two different primer pairs. Founder animals were intercrossed with C57BL/6 mice to establish lines.

Transgenic mice were screened with oligonucleotides tau-I (O-100, 5′-GGAGTTCGAAGTGATGGAAG-3′) and tau-K (O-101, 5′-GGTTTTT-GCTGGAATCCTGG-3′) and yielded an amplification product of 500 base pairs. A restriction digest of the amplification product by *Sma*I confirmed the presence of the P301L transgene. Ten independent transgenic lines were generated, four of which had comparable expression levels as determined by immunoblot analysis.

Antibodies—Antibody HT7 (Innogenetics Inc.; amino acids 159–163, diluted 1:400) was used to detect human tau specifically; tau-1 (Roche Molecular Biochemicals) was used to detect both human and murine tau on immunoblots; AT8 (Innogenetics Inc.; diluted 1:20) was used to detect tau phosphorylated at epitopes serine 202 and threonine 205; AT100 (Innogenetics Inc.; diluted 1:100) was used to detect tau phosphorylated at serine 212 and threonine 214; AT180 (Innogenetics Inc.; diluted 1:50) was used to detect tau phosphorylated at threonine 231 and serine 235; 12E8 (Dr. Peter Seubert, Elan Pharmaceuticals; diluted 1:100) was used to detect tau phosphorylated at serines 262 and 356; conformation-dependent antibody TG3 (Dr. Peter Davies; diluted 1:20) was used to detect tau phosphorylated at threonine 231 and serine 235; PHF1 (Dr. Peter Davies; diluted 1:50) was used to detect tau phosphorylated at serine 396 and serine 404; AD2 (Dr. Chantal Mourton-Gilles; diluted 1:500) was used to detect tau phosphorylated at serine 396 and serine 404; AD199 (Dr. A. Delacourte; diluted 1:1000; Ref. 9) was used

* The costs of publication of this article were defrayed in part by the payment of page charges. This article must therefore be hereby marked "*advertisement*" in accordance with 18 U.S.C. Section 1734 solely to indicate this fact.

‡ To whom correspondence should be addressed: Division of Psychiatry Research, University of Zürich, August Forel Strasse 1, 8008 Zürich, Switzerland. Tel: 41-1-634-8873; Fax: 41-1-634-8874; E-mail: goetz@bli.unizh.ch.

[1] The abbreviations used are: 4R, four-repeat; 3R, AD, Alzheimer's disease; TUNEL, terminal deoxynucleotidyl transferase-mediated biotinylated dUTP nick end-labeling; PBS, phosphate-buffered saline; TBS, Tris-buffered saline; S1, somatosensory cortex 1; M1, motor cortex 1; CA, cornu ammonis.

to detect tau phosphorylated at serine 199; MC1 (Dr. Peter Davies; diluted 1:10) was used to detect the conformational ALZ50 epitope; and rabbit anti-glial fibrillary acidic protein IgG (Sigma, catalog no. G-9269; diluted 1:400) was used to detect activated astrocytes. For peroxidase and diaminobenzidine stainings, secondary antibodies were obtained from Vector Laboratories (Vectastain ABC kits PK-6101 and PK-6102). For immunofluorescence, secondary antibodies were obtained from Molecular Probes (ALEXA-FLUOR series).

Immunoblot Analysis—Brains from transgenic and control mice (aged 3 weeks to 8 months) were weighed and Dounce homogenized in 2.5% (v/v) perchloric acid in phosphate-buffered saline (PBS), allowed to stand on ice for 30 min, and centrifuged for 10 min at 10,000 × *g*. The supernatants were dialyzed against 50 mM Tris-HCl (pH 7.4), 1 mM dithiothreitol, and 0.1 mM phenylmethylsulfonyl fluoride and used for immunoblot analysis as described, using equal amounts except for ALZ17, for which only half the amount of extract has been used (10). Ponceau staining of the membranes was included to confirm loading of comparable amounts of protein.

Sarcosyl extractions were done as described (10). In brief, brain tissue of 8-month-old pR5 transgenic and control mice were homogenized in 10 volumes of buffer consisting of 10 mM Tris-HCl (pH 7.4), 0.8 M NaCl, 1 mM EGTA, and 10% sucrose. An Alzheimer's disease (AD) brain sample was included as control. The homogenate was spun for 20 min at 20,000 × *g*. The supernatant was brought to 1% *N*-lauroylsarcosinate (Fluka, no. 61744), and incubated 1 h at room temperature while shaking. After a 1-h spin at 100,000 × *g*, the sarcosyl-insoluble pellets were resuspended in 50 mM Tris-HCl (pH 7.4) and stored at 4 °C. This material was used for both immunoblot analysis and electron microscopy.

Samples were run on 10% SDS-polyacrylamide gels and electrophoretically transferred to a nylon membrane (Hybond-ECL, Amersham Pharmacia Biotech). Residual protein-binding sites were blocked by incubation with 5% semifat dried milk in Tris-buffered saline (TBS) and 0.1% Tween 20 for 1 h at room temperature, followed by a 3-h incubation at room temperature with the primary antibody in TBS and 0.1% Tween 20, 1% semifat dried milk, and 0.02% sodium azide. Antibodies Tau-1 and HT7 were diluted 1:5000 and 1:250, respectively. After four washes for a total of 30 min in TBS, the membrane was incubated with a horseradish peroxidase-linked sheep anti-rabbit Ig (Amersham, NA931) at 1:5000 dilutions for 1 h at room temperature, followed by a 30-min wash in TBS. The membrane was then incubated for 1 min in ECL reagent (Vector Laboratories), excess liquid was removed, and the membrane was exposed to x-ray films. For reuse, membranes were stripped for 30 min at 50 °C in 100 mM 2-mercaptoethanol and 2% SDS in 62.5 mM Tris (pH 6.8).

Immunohistochemistry and TUNEL Staining—Brains from 3–4-month-old pR5 transgenic mice and an equal number of control mice (nontransgenic and wild-type human tau transgenic ALZ17 mice; Ref. 11) were used for immunohistochemical analysis. Animals were perfused transcardially with 4% paraformaldehyde in saline and sodium phosphate buffer (pH 7.4). Immunohistological, hematoxylin-eosin, and combined Holmes and Luxol stainings were done on 4-μm paraffin sections from brain and spinal cord by using standard published procedures (12). Some of the sections were pretreated with 5 μg/ml proteinase K in TBS or PBS at 37 °C for 2.5 min for signal enhancement. Sections were dehydrated in an ascending series of ethanol and flat embedded between glass slides and coverslips in Eukitt (Kindler). Sections were stained with thioflavin-S and silver impregnated by Gallyas (13) and modified Bielschowsky (14) protocols (15).

TUNEL Staining—To detect cells undergoing apoptosis, the peroxidase *in situ* cell death detection kit (Roche Molecular Biochemicals, no. 1684817) was used. In brief, paraffin-embedded sections were rehydrated, treated with 5 μg/ml proteinase K in PBS for 10 min at 37 °C, washed with ice-cold PBS four times, incubated in 3% H_2O_2 in methanol for 5 min at room temperature, and washed again. For a positive control, sections were incubated in 100 μg/ml DNase I (Roche Molecular Biochemicals, no. 104132) in 20 mM Tris-HCl (pH 8.0) and 10 mM $MgCl_2$ for 10 min at room temperature. Then, the labeling solution containing the enzyme terminal deoxynucleotidyl transferase (POD kit) was diluted 1:10 and added to the sections for 30 min at 37 °C. For a negative control, the enzyme was omitted from the labeling solution. Sample sections were washed, blocked with 2% bovine serum albumin, and incubated with convert solution (POD kit), washed again, and incubated in 1:10 diluted diaminobenzidine solution (Pierce, no. 1856090) for 10 min at room temperature to visualize the DNA breaks. Sections were dehydrated and mounted in Eukitt. To correlate numbers of HT7-positive neurons with glial fibrillary acidic protein-positive astrocytes and TUNEL reactivity, positive cells in an area of 0.7 × 0.6 mm of the somatosensory cortex S1 and the motor cortex M1 were counted in 10 sections per animal.

Electron Microscopy and Immunogold Electron Microscopy—Resuspended sarcosyl-insoluble material obtained from brains of transgenic mice, control mice, and an AD patient were placed directly on carbon-coated, 300-mesh grids, stained with 2% phosphotungstic acid, and analyzed by electron microscopy (see below). Samples were also processed for immunogold electron microscopy and incubated with the primary antibody in PBS and 0.1% gelatin for 90 min at room temperature. Antibody AT100 was used at 1:100 dilutions, antibody AT180 at 1:5 dilutions, rabbit antiserum AD199 at 1:50 dilutions, and hybridoma supernatant TG3 undiluted. As negative controls, filament preparations from AD brain and transgenic mice were incubated with α-synuclein-specific antiserum PER4 as well as an antibody against a PR8 influenza virus surface antigen. In addition, controls were included, in which the primary antibody had been omitted. Incubations were placed on Formvar- and carbon-coated, 300-mesh grids and allowed to evaporate partially. Grids were washed twice in PBS and 0.1% gelatin and incubated with the respective secondary antibody conjugated to 6 nm Au (Sigma) for 30 min in a humid chamber at room temperature. After two washes in PBS and 0.1% gelatin and one in water, the grids were blotted, stained with 2% phosphotungstic acid, and allowed to air dry. Micrographs were recorded at an operating voltage of 80–100 kV and at nominal magnifications of × 88,000 and × 175,000 on a Philips CM12 electron microscope.

RESULTS

Overexpression of Human tau—The neuron-specific elements of the mouse Thy1.2 promoter were used to express the longest human four-repeat tau isoform containing the two amino-terminal exons 2 and 3 (2^+3^+4R), along with human pathogenic mutation P301L (pR5 construct). Ten founders were obtained, four of which were used for further analysis on the basis of their expression levels: By immunoblot analysis of similar amounts of perchloric acid-soluble protein extracts, as judged by Ponceau stainings, a strong immunoreactive 66-kDa protein that corresponded to the transgenic tau band was identified in animals of some pR5 lines; it reacted with the anti-tau antibody Tau-1 that recognizes both human and murine tau (Fig. 1*A*), as well as with antibody HT7 against human, but not murine, tau (Fig. 1*B*). Soluble tau brain tissue levels for line pR5-183 were ~70% of endogenous tau (Fig. 1*A, lane 4*, *upper* transgenic *band* representing human tau compared with *lower bands* representing the endogenous murine tau isoforms). As expected, transgenic tau was absent from the wild-type brain protein extracts (Fig. 1*B, lane 8*). Amounts of sarcosyl-insoluble tau (Fig. 1*C*) were generally higher in the pR5-183 (Fig. 1*C, lane 1*) than in our transgenic mice that expresses human tau without the mutation (ALZ17 line; Ref. 11; Fig. 1*C, lane 3*). Protein extracts from pR5-183 mice were therefore subsequently used for electron microscopy. The transgenic mutant tau in pR5-183 mice was hyperphosphorylated, as indicated by several phosphorylation-dependent anti-tau antibodies (data not shown).

To determine the distribution and localization of tau in brain, a 3-month-old mouse of the pR5-183 line was analyzed by immunohistochemistry using antibody HT7. Expression levels of human tau were high in hippocampus, fornix fimbriae, amygdala, spinal cord, and cortex (Fig. 2*A*), weaker in brain stem and striatum, and not detectable in olfactory bulb and cerebellum. A sagittal section of the hippocampus showed numerous HT7-positive pyramidal neurons in the CA1 region but not in CA3. The mossy fiber projections of the hippocampus were strongly stained, whereas staining intensity was somewhat weaker in dentate gyrus granule cells (Fig. 2, *A* and *C*). In CA1 pyramidal neurons human tau was present in axons but accumulated also in cell bodies and apical dendrites (Fig. 2*B*). In brain stem, HT7-positive cells were identified, in addition to axonal spheroids, and cells that expressed tau were strongly stained, with granular accumulation of tau (Fig. 2*D*). In addition, a subset of pyramidal cells in the cerebral cortex was HT7

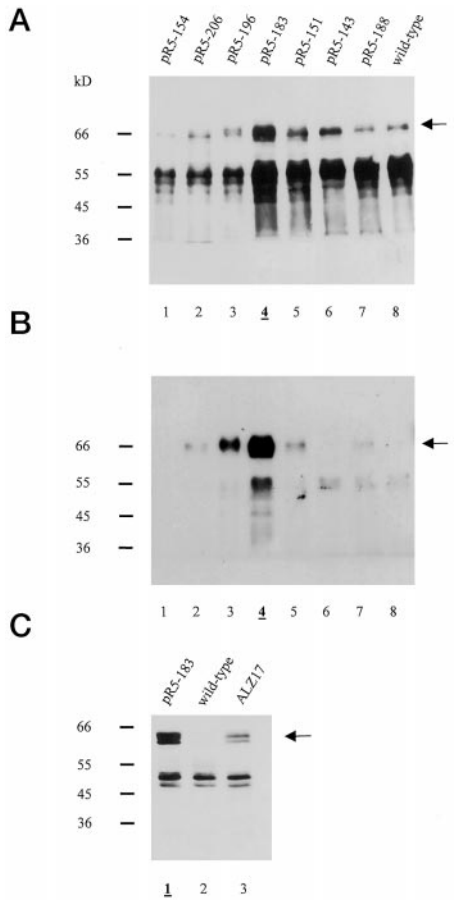

FIG. 1. **Immunoblot analysis of tau protein in brains from mice of pR5 lines.** *A*, tau protein extracted with perchloric acid from brains of different 3-month-old mice of pR5 lines (*lanes 1–7*; *lane 4*, line pR5-183) and a wild-type control mouse (*lane 8*) was analyzed by immunoblotting using anti-tau antibody Tau-1. This antibody recognizes murine and human tau. *B*, the blot was stripped and reprobed with HT7, a human tau-specific antibody. The *arrow* points to the human tau band. *C*, sarcosyl-insoluble tau from the brains of 8-month-old mice of line pR5-183 (*lane 1*), a wild-type control mouse (*lane 2*), and a wild-type human tau transgenic ALZ17 mouse (*lane 3*) analyzed by immunoblotting using antibody HT7. The *arrow* points to the human tau band.

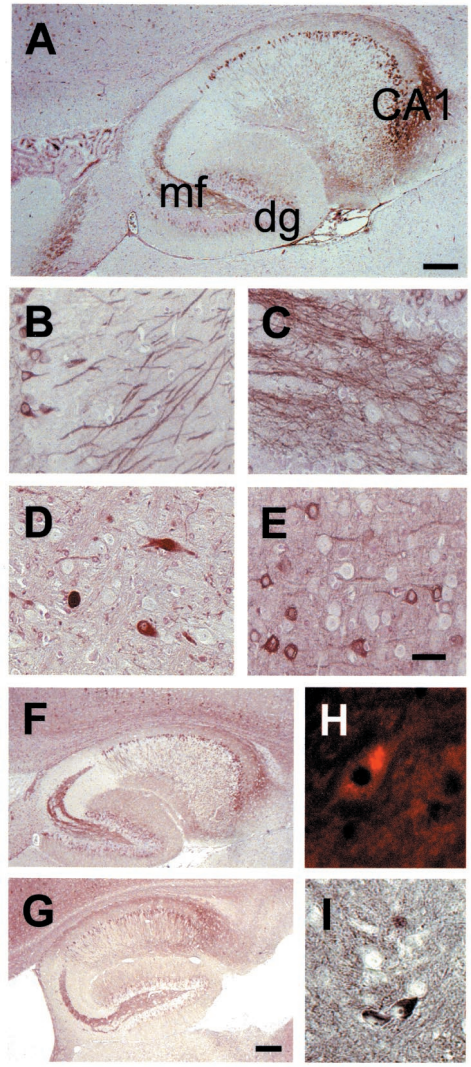

FIG. 2. **Tau immunoreactivity in brain from a 3-month-old mouse of the pR5 line reveals high expression of human tau.** *A*, sagittal section of the hippocampus shows HT7-positive pyramidal neurons in CA1. Staining is less intense for dentate gyrus (*dg*) granule cells. Also note strong immunostaining of the mossy fiber (*mf*) projection in sector CA3 of the hippocampus. *B*, CA1 pyramidal neurons accumulate human tau in cell bodies and apical dendrites. *C*, the mossy fiber network is intensely stained, revealing transport of human tau into the axon. *D*, In brain stem, HT7-positive cells are found with granular accumulation of tau, in addition to axonal spheroids. *E*, in cerebral cortex, a subset of pyramidal cells is HT7-immunoreactive. Note the intense, granular immunostaining of cell bodies and dendrites. No immunoreactivity was observed in control mice. *F* and *G*, staining of cell bodies and dendrites of dentate gyrus granule cells with antiserum AD199 is less pronounced in pR5-183 mice (*F*) compared with wild-type human tau transgenic ALZ17 mice (*G*). *H* and *I*, neurofibrillary tangles are identified in several brain areas including spinal cord by thioflavin-S fluorescent microscopy (*H*) and Gallyas silver stains (*I*). *Scale bars*: *A, F*, and *G*, 100 μm; *B–E*, 20 μm.

immunoreactive. As for CA1 pyramidal cells, we found granular immunostaining of cell bodies and dendrites (Fig. 2*E*). In comparison with wild-type human tau transgenic ALZ17 mice, staining of cell bodies and dendrites of the dentate gyrus granule cells was less pronounced in pR5-183 mice, as determined with antiserum AD199 (Fig. 2, *F* and *G*) or antibody HT7 (data not shown). In other brain areas, staining patterns were comparable. Neurofibrillary tangles were identified in spinal cord, brain stem, and cortical layers 5 and 6 by thioflavin-S fluorescent microscopy (Fig. 2*H*) and Gallyas silver stains (Fig. 2*I*).

Abnormal Phosphorylation and Conformation of tau—To determine the phosphorylation status of tau in 3-month-old pR5 mice, we used a panel of phosphorylation- and conformation-dependent anti-tau antibodies. Antibody TG3, a phosphorylation- and conformation-dependent antibody, stained pyramidal neurons of the CA1 region of the hippocampus of transgenic mice (Fig. 3*A*) but not controls (Fig. 3*B*). TG3 stained numerous pyramidal neurons in cortices of transgenic (Fig. 3*C*) but not control (Fig. 3*D*) mice. The conformation-dependent antibody MC1 that detects the ALZ50 epitope of AD tau stained pyramidal neurons of the CA1 region and the cortex of transgenic (Fig. 3, *E* and *G*) but not control (Fig. 3, *F* and *H*) mice. The same staining pattern was obtained with antibody AT180, which detects tau phosphorylated at threonine 231 and serine 235 (Fig. 3, *I–M*). Antibody AD199 directed against phosphorylated serine 199 stained hippocampal and cortical neurons moderately, antibody AT8 directed against serines 202 and 205 stained only weakly and was mainly restricted to cortical neurons, whereas antibodies AD2 and PHF1 directed against serines 396 and 404 did not detect any neurons. Staining with antibodies 12E8 and AT100 revealed similar patterns in transgenic and control mice (data not shown).

Astrocytosis and Apoptosis—To detect activated astrocytes, we used an antibody against glial fibrillary acidic protein. This

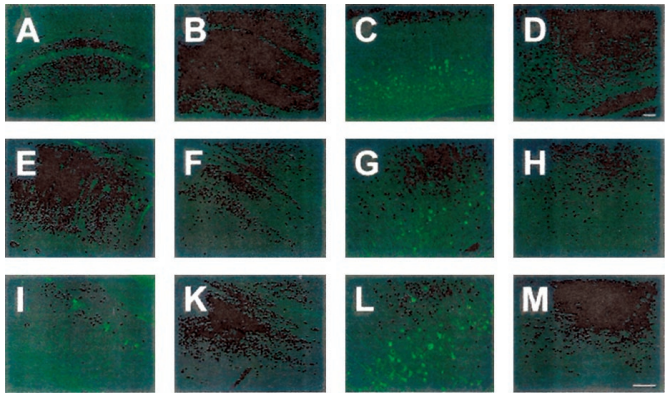

FIG. 3. **Tau phosphorylation and conformational changes in P301L tau transgenic mice.** Antibody TG3, a phosphorylation- and conformation-dependent antibody, stains pyramidal neurons of the CA1 region of the hippocampus of transgenic mice (*A*), but not controls (*B*). Also in cortex, numerous pyramidal neurons are stained by this antibody in transgenic mice (*C*), but not controls (*D*). The conformation-dependent antibody MC1 stains pyramidal neurons of the CA1 region and the cortex of transgenic mice (*E* and *G*) but not controls (*F* and *H*). The same staining pattern is obtained with phosphorylation-dependent antibody AT180 (*I–M*). *Scale bars*: *A–D*, 30 μm; *E–M*, 30 μm.

antibody revealed activated astrocytes in the amygdala and in cortical areas of transgenic mice that contained numerous tau-positive neurons (Fig. 4*A*). No such activated astrocytes were observed in control amygdala and cortex (Fig. 4*B*). Also, no astrocyte activation was found in the hippocampus of transgenic mice (data not shown). To identify cells that underwent apoptosis, we used TUNEL stains and found many TUNEL-positive neurons in the somatosensory cortex that contained numerous tau-positive neurons (Fig. 5*A*). By contrast, only very few TUNEL-positive cells were present in wild-type mice, and staining was faint compared with transgenic mice (Fig. 5*B*). As negative control, we omitted the POD convert solution (Fig. 5*C*), and, as a positive control, we pretreated sections with DNase I (Fig. 5*D*). No TUNEL-positive neurons were identified in the hippocampus of transgenic mice (data not shown). We correlated numbers of HT7-positive neurons with glial fibrillary acidic protein-positive astrocytes and TUNEL reactivity in the somatosensory cortex and counted per visual field 50 (±14) HT7-positive neurons, 19 (±6) activated astrocytes, and 7 (±3) dark TUNEL-positive cells in transgenic brain compared with no HT7-positive neurons, 5 (±2) activated astrocytes, and 3 (±3) faint TUNEL-positive cells in the wild-type control (Fig. 4*C*). To correlate astrocytosis and tau expression in different brain areas, we compared in transgenic brain motor cortex M1 and somatosensory cortex S1 and counted per visual field 14 (±4) HT7-positive neurons and 5 (±1) activated astrocytes in the M1 cortex compared with 50 (±14) HT7-positive neurons and 19 (±6) activated astrocytes in the S1 cortex (Fig. 4*D*).

Tau Filaments—We prepared sarcosyl protein extracts for electron microscopy analyses in parallel from brain tissue of an AD patient, 8-month-old pR5 transgenic mice, and control mice and found tau filaments in both AD and transgenic mouse brains. The tau filaments in AD brain had a width of ~20 nm (Fig. 6, *A* and *B*), and those in transgenic mice were ~15 nm wide and significantly shorter (Fig. 6*C*). No such filaments were present in any of the control mice (data not shown). To identify phosphoepitopes of tau, we incubated the filaments with a panel of phosphorylation-dependent antibodies. Immunogold electron microscopy of extracts obtained from AD (Fig. 6, *D* and *F*) and pR5 transgenic (Fig. 6, *E* and *G*) brains using TG3 (Fig. 6, *D* and *E*) or AT8 (Fig. 6, *F* and *G*) identified several 6-nm, gold-decorated filaments. These filaments were also stained by the antibodies AT100 and AD199 (data not shown).

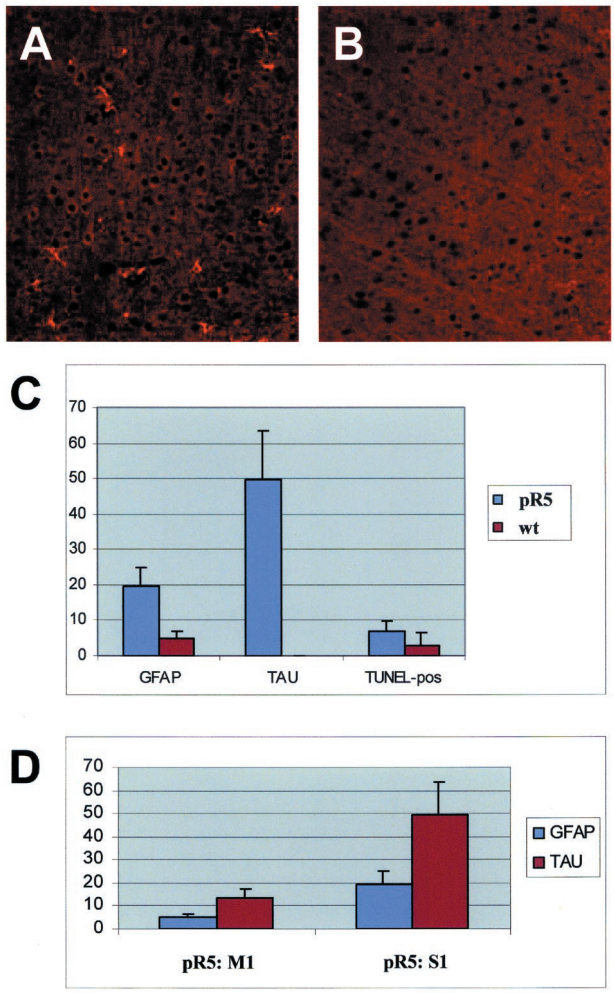

FIG. 4. *A*, activated astrocytes are detected in those cortical areas of transgenic mice that contain numerous tau-positive neurons. *B*, no such activated astrocytes are found in control cortex. *C* and *D*, In the somatosensory cortex S1, 50 (±14) HT7-positive neurons, 19 (±6) activated astrocytes, and 7 (±3) dark TUNEL-positive cells are present per visual field in transgenic brains, compared with no HT7-positive neurons, 5 (±2) activated astrocytes, and 3 (±3) faint TUNEL-positive cells in wild-type controls (*C*). Astrocytosis and tau expression are positively correlated in different brain areas of transgenic mice: per visual field, 14 (±4) HT7-positive neurons and 5 (±1) activated astrocytes are present in the M1 cortex, compared with 50 (±14) HT7-positive neurons and 19 (±6) activated astrocytes in the S1 cortex (*D*).

In AD brains, tau filaments consist of two structurally distinct parts, the core and the fuzzy coat. The known, darkly stained space between the filaments and the gold particles typically corresponds to the known fuzzy coat of the filaments (10, 16). No filaments were identified or decorated by gold-labeled antibodies in negative controls, proving the specificity of these antibodies. In particular, we found no neurofilaments, with a width of 10 nm and an axial periodicity of 21 nm in the preparation (17).

DISCUSSION

The results of this study show that transgenic expression of human P301L mutant tau under control of the murine Thy1.2 genomic expression vector leads to the formation of sarcosyl-insoluble, 15-nm-wide tau filaments. By comparison, tau filaments in frontotemporal dementia with parkinsonism linked to chromosome 17 patients with the P301L mutation (Dutch family 1) consist of 15-nm-wide, slender, twisted filaments with variable periodicity, in addition to a few straight filaments (1),

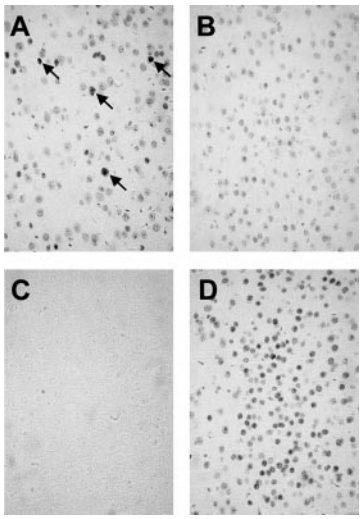

FIG. 5. **TUNEL staining reveals neurons undergoing apoptosis in transgenic mice.** *A* and *B*, in cortical areas of transgenic mice that contain numerous tau-positive neurons, many TUNEL-positive neurons are identified (*A*), which are absent from controls (*B*). *Arrows* point to some positive neurons. *C* and *D*, negative control without reagent (*C*) and positive control, pretreated with DNase I (*D*).

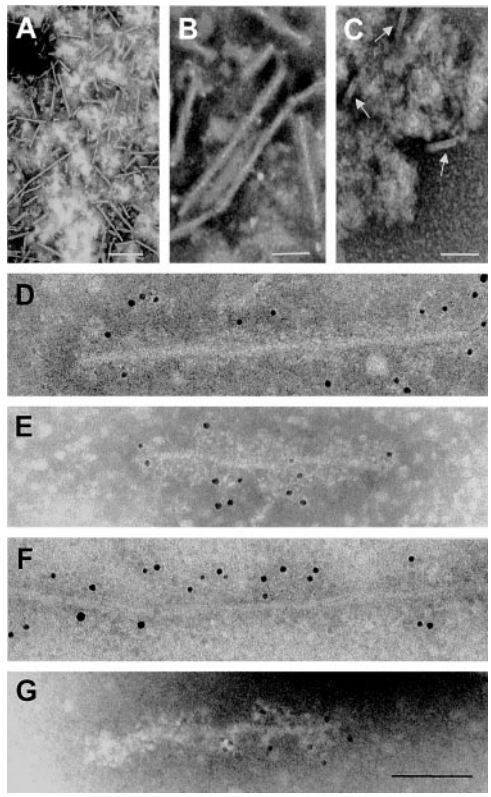

FIG. 6. **Neuronal tau filaments in 8-month-old P301L tau transgenic brain revealed by electron microscopy and immunogold electron microscopy of sarcosyl extracts.** *A* and *B,* tau filaments in an extract obtained from an AD brain have a width of ~20 nm. *C*, Tau filaments in an extract obtained from the pR5 brain are shorter and have a width of ~15 nm (*arrows*). No such filaments were identified in sarcosyl extracts of control mice. *D* and *E*, immunogold electron microscopy of extracts obtained from AD (*D*) and pR5 brain (*E*) using phosphorylation- and conformation-dependent antibody TG3 identifies 6-nm, gold-decorated filaments. *F* and *G*, immunogold electron microscopy of extracts obtained from AD (*F*) and pR5 brain (*G*) using phosphorylation-dependent antibody AT8 also identifies 6-nm, gold-decorated filaments. *Scale bars*: *A*, 400 nm; *B* and *C*, 80 nm; *D*–*G*, 80 nm.

and the tau filaments obtained from AD brains consist of 20-nm-wide, paired helical or straight filaments. The filaments in our P301L tau transgenic mice have the same width as those in the human disease associated with the P301L mutation (Dutch family 1). They were, however, shorter than filaments enriched from AD brains, which we included as positive control because of the unavailability of a brain sample from Dutch family 1. One likely explanation for the prevalence of short filaments in our mice is that the longest tau isoform expressed in our mouse contained two calpain recognition motifs for proteolytic degradation that may favor the formation of shorter filaments. In addition to the P301L mutation, the filament formation in our mice may also be related to high expression levels achieved by using the murine Thy1.2 expression vector, as shown by immunoblot analyses. A possible contribution of high expression levels to tau filament formation in our mouse lines is supported by the concentration dependence of filament assembly *in vitro* that resembles a nucleation-dependent process (18, 19). Together, the failure of previous attempts to model tau filament formation in transgenic mice may be related to either the absence of disease-causing mutations in the expression constructs or low expression levels (11, 20–25) or both.

In our mice, the murine Thy1.2 promoter directed expression of tau mainly to hippocampal and cortical neurons. Brain regions, which in human disease are spared from tau pathology, such as the cerebellum, did not express detectable levels of tau, as determined by immunofluorescence. As in human tauopathies (26), tau accumulated not only in axons but also in cell bodies and dendrites. To establish phosphoepitopes that are related to tau aggregation and filament formation, we used a panel of phosphorylation-dependent antibodies. In brains from patients of Dutch family 1, phosphorylation-dependent antibodies AT8, AT100, AT180, AT270, PHF1, and 12E8 stained numerous deposits in several brain regions, including the cortex, the dentate gyrus, and the CA1 region of the hippocampus. These deposits were mainly of the pretangle type and located in the perinuclear region and cell body and sometimes extended to the apical dendrites of neurons (1). In our model, AT100 and 12E8 did not discriminate wild-type from transgenic mice. AT8 staining was weak in transgenic mice and mainly restricted to a subset of cortical neurons, where it was found not only in cell bodies but also in dendrites. AT100 and PHF1 did not stain any neuron at up to 6 months of age. Age may account for this apparent difference between human disease and the mouse model, especially because filaments obtained from 8-month-old transgenic mice were AT100- and AT8-positive. AT180 and also the conformation-dependent antibodies MC1 and TG3, which were not included in the human study, revealed strong somatodendritic staining in both cortical and hippocampal pyramidal neurons of transgenic mice. Antibodies MC1 and TG3 recognize a distinct pathological conformation of the tau molecule in AD. In normal autopsy-derived brain tissue, tau is not stained by these antibodies. Our data indicate that transgenic tau underwent a conformational change favoring filament formation. Indeed, by immunogold electron microscopy of sarcosyl-insoluble tau protein, the AT8, AD199, AT100, and TG3 epitopes were identified on tau filaments in our P301L transgenic mice. For comparison, in the human study only one antibody, AT8, was used that labeled tau filaments (1). The distance of the gold particles from the core of the filament is similar to that reported for AD filaments (10). The space between the filaments and the gold particles corresponds to the known fuzzy coat of the filaments (10, 16). Taken together, tau in the nonfilamentous and filamentous states is hyperphosphorylated at several sites, which are also hyperphosphorylated in human tauopathies.

In Dutch family 1, neurological examination of brains revealed gliosis and severe neuronal loss in frontal and temporal

cortex and variable loss in the parietal cortex, whereas the hippocampus showed only mild to moderate neuronal loss and gliosis (1). These data are consistent with our findings. Despite comparable levels and phosphorylation of human tau in hippocampus and cortex of transgenic mice, we found evidence for apoptosis and astrocytosis in cortical areas and in the amygdala but not in the hippocampus. Astrocytosis was positively correlated with levels of human tau expression, as shown for the M1 and S1 cortices. Therefore, we cannot exclude the possibility that this pathology progresses and will include the hippocampus with advanced aging in older mice.

Together, our data show that the P301L mutation in combination with high expression levels can cause the formation of abnormal tau filaments in neurons in mice. Filament formation was also reported recently in mice expressing $2^{-}3^{-}4$R tau, along with the human pathogenic mutation P301L, under control of the mouse prion protein promoter. These mice show an advanced neurological phenotype, likely reflecting differences between $2^{-}3^{-}4$R and $2^{+}3^{+}4$R tau (27). In our P301L mice, filaments were phosphorylated at distinct epitopes, and their formation was accompanied by astrocytosis and apoptosis. These data indicate that P301L is a key pathogenic factor, and they underscore its pathophysiological role in frontotemporal dementia with parkinsonism linked to chromosome 17. Moreover, our results suggest the use of these mice, either alone or in combination with a pathogenic APP mutation, for the study of both the pathophysiology and the prevention of tau filament formation in neurodegenerative diseases.

Acknowledgments—We thank Daniel Schuppli, Eva Moritz, Yves Santini, and James Opoku for excellent technical assistance. We thank Dr. Thomas Baechi for providing the electron microscopy facility and members of his laboratory, in particular Ruth Keller and Hans-Peter Gautschi, for assistance. We thank Dr. Peter Davies for antibodies TG3, MC1, and PHF1, Dr. A. Delacourte for antiserum AD199, Dr. Peter Seubert (Elan Pharmaceuticals) for antibody 12E8, and Drs. Michel Goedert and Ross Jakes for rabbit anti-α-synuclein antiserum PER4.

REFERENCES

1. Spillantini, M. G., Crowther, R. A., Kamphorst, W., Heutink, P., and van Swieten, J. C. (1998) *Am. J. Pathol.* **153,** 1359–1363
2. Goedert, M., and Jakes, R. (1990) *EMBO J.* **9,** 4225–4230
3. Brandt, R., and Lee, G. (1994) *Cell Motil. Cytoskeleton* **28,** 143–154
4. Trinczek, B., Ebneth, A., Mandelkow, E. M., and Mandelkow, E. (1999) *J. Cell Sci.* **112,** 2355–2367
5. Goedert, M., Spillantini, M. G., Jakes, R., Crowther, R. A., Vanmechelen, E., Probst, A., Gotz, J., Burki, K., and Cohen, P. (1995) *Neurobiol. Aging* **16,** 325–334
6. Iqbal, K., Alonso, A. C., Gong, C. X., Khatoon, S., Pei, J. J., Wang, J. Z., and Grundke-Iqbal, I. (1998) *J. Neural. Transm. Suppl.* **53,** 169–180
7. Grover, A., Houlden, H., Baker, M., Adamson, J., Lewis, J., Prihar, G., Pickering-Brown, S., Duff, K., and Hutton, M. (1999) *J. Biol. Chem.* **274,** 15134–15143
8. Varani, L., Hasegawa, M., Spillantini, M. G., Smith, M. J., Murrell, J. R., Ghetti, B., Klug, A., Goedert, M., and Varani, G. (1999) *Proc. Natl. Acad. Sci. U. S. A.* **96,** 8229–8234
9. Sergeant, N., Wattez, A., and Delacourte, A. (1999) *J. Neurochem.* **72,** 1243–1249
10. Goedert, M., Spillantini, M. G., Cairns, N. J., and Crowther, R. A. (1992) *Neuron* **8,** 159–168
11. Probst, A., Gotz, J., Wiederhold, K. H., Tolnay, M., Mistl, C., Jaton, A. L., Hong, M., Ishihara, T., Lee, V. M., Trojanowski, J. Q., Jakes, R., Crowther, R. A., Spillantini, M. G., Burki, K., and Goedert, M. (2000) *Acta Neuropathol. (Berl.)* **99,** 469–481
12. Gotz, J., Probst, A., Ehler, E., Hemmings, B., and Kues, W. (1998) *Proc. Natl. Acad. Sci. U. S. A.* **95,** 12370–12375
13. Gallyas, F. (1971) *Acta Morphol. Acad. Sci. Hung.* **19,** 1–8
14. Yamamoto, T., and Hirano, A. (1986) *Neuropathol. Appl. Neurobiol.* **12,** 3–9
15. Probst, A., Tolnay, M., Langui, D., Goedert, M., and Spillantini, M. G. (1996) *Acta Neuropathol. (Berl.)* **92,** 588–596
16. Wischik, C. M., Novak, M., Edwards, P. C., Klug, A., Tichelaar, W., and Crowther, R. A. (1988) *Proc. Natl. Acad. Sci. U. S. A.* **85,** 4884–4888
17. Heins, S., Wong, P. C., Muller, S., Goldie, K., Cleveland, D. W., and Aebi, U. (1993) *J. Cell Biol.* **123,** 1517–1533
18. Perez, M., Valpuesta, J. M., Medina, M., Montejo de Garcini, E., and Avila, J. (1996) *J. Neurochem.* **67,** 1183–1190
19. Goedert, M., Jakes, R., Spillantini, M. G., Hasegawa, M., Smith, M. J., and Crowther, R. A. (1996) *Nature* **383,** 550–553
20. Gotz, J., Probst, A., Spillantini, M. G., Schafer, T., Jakes, R., Burki, K., and Goedert, M. (1995) *EMBO J.* **14,** 1304–1313
21. Goedert, M., and Hasegawa, M. (1999) *Am. J. Pathol.* **154,** 1–6
22. Brion, J. P., Tremp, G., and Octave, J. N. (1999) *Am. J. Pathol.* **154,** 255–270
23. Ishihara, T., Hong, M., Zhang, B., Nakagawa, Y., Lee, M. K., Trojanowski, J. Q., and Lee, V. M. (1999) *Neuron* **24,** 751–762
24. Spittaels, K., Van den Haute, C., Van Dorpe, J., Bruynseels, K., Vandezande, K., Laenen, I., Geerts, H., Mercken, M., Sciot, R., Van Lommel, A., Loos, R., and Van Leuven, F. (1999) *Am. J. Pathol.* **155,** 2153–2165
25. Duff, K., Knight, H., Refolo, L. M., Sanders, S., Yu, X., Picciano, M., Malester, B., Hutton, M., Adamson, J., Goedert, M., Burki, K., and Davies, P. (2000) *Neurobiol. Dis.* **7,** 87–98
26. Delacourte, A., David, J. P., Sergeant, N., Buee, L., Wattez, A., Vermersch, P., Ghozali, F., Fallet-Bianco, C., Pasquier, F., Lebert, F., Petit, H., and Di Menza, C. (1999) *Neurology* **52,** 1158–1165
27. Lewis, J., McGowan, E., Rockwood, J., Melrose, H., Nacharaju, P., Van Slegtenhorst, M., Gwinn-Hardy, K., Paul Murphy, M., Baker, M., Yu, X., Duff, K., Hardy, J., Corral, A., Lin, W. L., Yen, S. H., Dickson, D. W., Davies, P., and Hutton, M. (2000) *Nat. Genet.* **25,** 402–405

Tau Filament Formation in Transgenic Mice Expressing P301L Tau

Jürgen Götz, Feng Chen, Robi Barmettler and Roger M. Nitsch

J. Biol. Chem. 2001, 276:529-534.
doi: 10.1074/jbc.M006531200 originally published online September 29, 2000
